Upper and Lower Limits of Human Skin Electrical Resistance in Iontophoresis

Steven M. Dinh, Ching-Wang Luo, and Bret Berner
Basic Pharmaceutics Research, Ciba-Geigy Corporation, Ardsley, NY 10502

The time-dependent electrical resistance of human cadaver skin was shown to be bound by an upper limit at equilibrium and a lower limit at steady state. The time to reach steady state from any initial condition by applying a current was much shorter than the recovery to equilibrium, due to different driving forces. The ratio of the equilibrium to the solution resistances increased with the salt concentration in free solution. This equilibrium relative resistance was sensitive to skin variability, primarily due to its dependence on porosity and pore geometry. A model was developed relating the equilibrium relative resistance to the structural properties of skin. The estimated pore radius of 25×10^{-10} m from the equilibrium resistance data is consistent with the average pore radius of human skin reported in the literature. In contrast, the steady-state resistance could be several orders of magnitude lower than the equilibrium resistance and depended on current density and salt concentration but not on the history of prior exposures of a skin sample to a current. This difference can greatly reduce the power requirement for iontophoresis and can make this technology more practical. A linear relationship was found between the logarithm of the steady-state relative resistance (skin/solution resistances) and the logarithm of the current density divided by the salt concentration. The slope of -0.65 was in excellent agreement with the theoretical slope of $-2/3$ that was derived for the convective transport of ions in a charged pore under a constant current.

Introduction

The goal of controlled drug delivery is to improve therapy by specifying the drug input to optimize the desired pharmacodynamic or biological response (Berner and Dinh, 1992). The transdermal route provides a readily accessible, safe and noninvasive site for introducing a drug directly into the systemic circulation, and thereby avoids the high first-pass metabolism of the drug by the liver. To reach the network of capillaries, a drug must cross the stratum corneum, the viable epidermis, and into the dermis. The stratum corneum is the surface layer of skin consisting of keratinized epithelial cells and comprises proteins dispersed in a continuum of lipid bilayers. Although its thickness is only about 20 μm, it is the principal barrier to permeation (Scheuplein and Blank, 1971). Michaels et al. (1975) provided a quantitative prediction of drug permeation across skin and showed that skin is much more permeable to nonionic drugs. Consequently, most of the research effort has been directed to developing transdermal systems for noncharged chemical entities.

Advances in genetic engineering have allowed for the mass production of peptides and proteins for a variety of therapies without adequate treatments. However, these peptides and proteins can be delivered only by the parental route, and patience convenience and compliance become an issue. Moreover, these large charged molecules and the smaller ionic drugs do not permeate readily across skin because of their low partitioning into the lipid matrix of the stratum corneum. Providing a solution to this transport problem without problems in cutaneous tolerability is a major challenge in transdermal drug delivery. At the same time, understanding the mechanisms of transport poses fundamental questions on the micromechanics of how charged molecules can be delivered across a predominantly lipophilic barrier.

Iontophoresis is an emerging technology for transdermal drug delivery, whereby a constant current, instead of a constant

Correspondence concerning this article should be addressed to S. M. Dinh.

electric field, is used to enhance and control primarily the delivery of charged compounds across skin. Designing an iontophoretic delivery system involves optimizing the transport of ionic drugs across skin and the electronics of the system. Both issues require understanding the electrical properties of skin. For instance, the voltage of a power source needed to produce a constant current is determined by the electrical resistances of the skin and the device components. In addition, drug transport can be optimized by elucidating the mechanisms of ionic transport across skin and the interactions between driving forces and resistances. As such, iontophoresis and controlled-release technology present intriguing and challenging problems that are ripe for fundamental analysis in transport phenomena.

The *in vitro* electrical properties of human skin were reported by a number of authors using various electrochemical techniques. DeNuzzio and Berner (1990) measured the resistance and capacitance of skin by impedance spectroscopy. The resistance was highly variable, with a typical value of $10^5\ \Omega$ (ohm) from a fresh skin sample. In contrast, the capacitance was less variable and was approximately $1-20\times10^{-9}$ F (farad). Kasting and Bowman (1990) used constant current measurements and reported a similar initial resistance. They further noted that the resistance decreased with increasing current or voltage. Foley et al. (1991) observed that, in constant current measurements, the capacitance did not change appreciably with time, whereas the resistance decreased precipitously with time. Since the electrical resistance of skin could change, learning how to control this resistance could significantly reduce power consumption and enable this technology to become more practical. The reported data were modeled by an electrical circuit (Tregear, 1966; Coster et al., 1992), consisting of a resistor connected in parallel to a capacitor. The resistance and the capacitance represented the dissipative and storage components, respectively. At a given temperature, the resistance data were more variable than the capacitance results (DeNuzzio and Berner, 1990; Kasting and Bowman, 1990; Foley et al., 1991) and appeared to depend on numerous variables, such as skin donor, applied current, ionic strength, and time. A second resistor was usually added in series to the parallel circuit element to depict the electrical resistance of the solvent.

Given the importance of understanding the electrical properties of skin to guide system design, a need arises to determine the functions of these independent variables systematically. The objective of this work is to demonstrate that the electrical resistance of skin is time-dependent and is bound by an upper limit at equilibrium and a lower limit at steady state.

Materials and Methods

The electrical properties of skin were characterized by impedance spectroscopy and constant current measurement. The apparatus, materials, and methods are summarized below.

Apparatus

The experimental apparatus used for impedance and constant current measurements is shown in Figure 1. The Solartron 1250/1286 system (Solartron Instruments, Burlington, MA) was used to generate an electrical input and measure the electrical response. A Solartron system was interfaced to a Hewlett Packard 9816 computer (Roseville, CA) for instrument control and data acquisition.

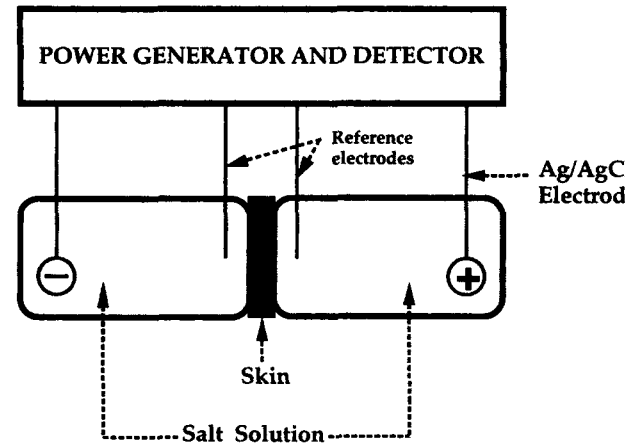

Figure 1. Experimental apparatus

The side-by-side four-electrode electrochemical setup, as shown in Figure 1, was made from two diffusion cells by Crown Glass (Somerville, NJ). The skin sample was clamped in the ground-glass joint separating the two cells, each cell volume was approximately 3 mL. The transport area of the skin sample was 0.7 cm^2. Temperature was maintained at 305 K by water-jacketing. Silver/silver chloride working and reference electrodes were used. The working and counterelectrodes were 5.57 cm apart, and the reference electrodes were separated by 2.22 cm. These electrodes were made by depositing electrochemically silver chloride on silver wires that were immersed in an aqueous solution of potassium chloride and hydrochloric acid.

Materials

Sodium chloride was used as received from Sigma Chemicals (Springfield, MO), and salt solutions were prepared with purified water (Millipore Filtration System, Millipore Company, Bedford, MA). The concentrations ranged from dilute (0.012 M) to saturated (6.1 M) salt solutions. For convenience, the units for concentration used in this work are molar (M), instead of mol/m^3 in SI units.

Skin preparation

Dermatomed human skin ($\sim$400 μm thick) was received frozen (203 K) from skin banks (New York Firefighters Skin Bank, New York, NY) and stored frozen until use. Samples were used immediately after thawing.

Impedance spectroscopy and constant current

The procedures for impedance and constant current measurements were described in detail elsewhere (DeNuzzio and Berner, 1990; MacDonald, 1981). Impedance spectroscopy was used to measure the "instantaneous" electrical properties of the skin sample. The frequency response analyzer was used in the range of 1–65,000 Hz at increments of 10 frequencies per logarithmic decade. The amplitude of the perturbing potential was 3 mV. The transient electrical response of skin under a constant current was determined by measuring the voltage, while a current was applied. Applied constant current densities ranging from 50–1,000 $\mu A/cm^2$ were investigated.

Procedures

In a typical experiment, the electrical resistance of a salt solution was measured in the diffusion cells without the skin sample present. A skin sample was then mounted between the diffusion cells. Each cell was filled with a salt solution of the same concentration to minimize axial diffusion across the skin. The volume of the salt solution was sufficiently large to maintain a constant concentration for the duration of the iontophoresis experiment. Prior to initiating the experiment, the skin sample was equilibrated in the salt solution for 24 h. An impedance measurement was taken at the end of the equilibration period. A constant current was then applied for 1 h. Voltage measurements were recorded during this period. At the end of this active segment, the impedance was measured. The impedance was again measured at the end of a rest period of 1 h. A constant current was then reapplied. The procedure to measure impedance at the beginning and end of each active segment was repeated. Hence, the effects of current density and salt concentration (or ionic strength) were evaluated systematically.

Results and Discussion

Transient resistance

The electrical resistance of skin, during the application of a constant current, was time-dependent, as shown in Figure 2. In this example, the applied current density was 200 $\mu A/cm^2$, and the NaCl concentration was 0.012 M. As depicted in Figure 2, the initial rise in resistance occurred in a short period of time, with a characteristic time less than 10^{-3} s. After reaching its peak value, the resistance gradually decreased to a steady-state value, with a characteristic time of approximately 10^3 s. Since the resistance is generally not unique, is the steady-state resistance reproducible in a given salt concentration and an applied current? To ascertain this question, a constant current was applied for 1 h (segment 1), turned off for 1 h, turned on for 1 h (segment 2), turned off for 1 h, and turned on for 1 h (segment 3). The results are shown in Figure 3, with the same applied current density of 200 $\mu A/cm^2$ and NaCl concentration of 0.012 M. The resistances that corresponded to segments 1, 2 and 3, as shown in Figure 3, followed separate time courses, but converged to the same steady-state value.

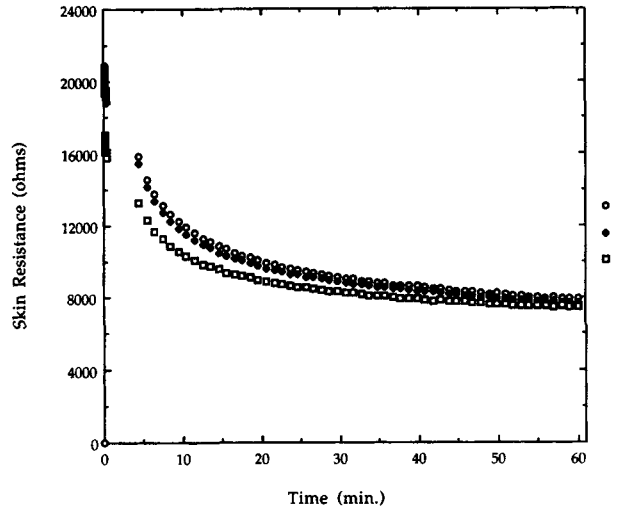

Figure 3. Approach to steady-state resistance from different initial conditions.

To demonstrate further the existence of a steady-state resistance, a different set of experimental conditions were investigated, where the applied current density was 600 $\mu A/cm^2$ and the NaCl concentration was 0.154 M. As shown in segment 1 of Figure 4a, the initial resistance of this skin sample, measured by impedance, was approximately 200,000 Ω. When a constant current density of 600 $\mu A/cm^2$ was applied, the resistance approached a steady-state value of approximately 1,800 Ω (segment 2 in Figure 4b). This steady-state resistance was verified by impedance measurement (segment 3 in Figure 4a) at the end of the constant current period of 1 h. After a test period of 1 h, the resistance of skin was partially recovered

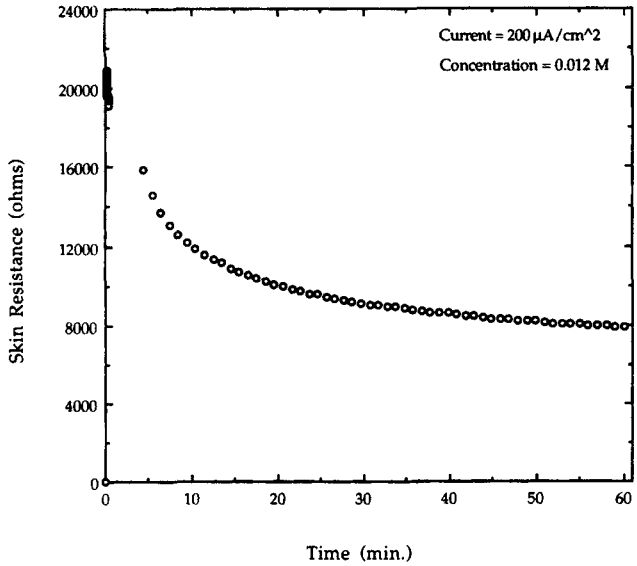

Figure 2. Transient behavior of skin electrical resistance during iontophoresis.

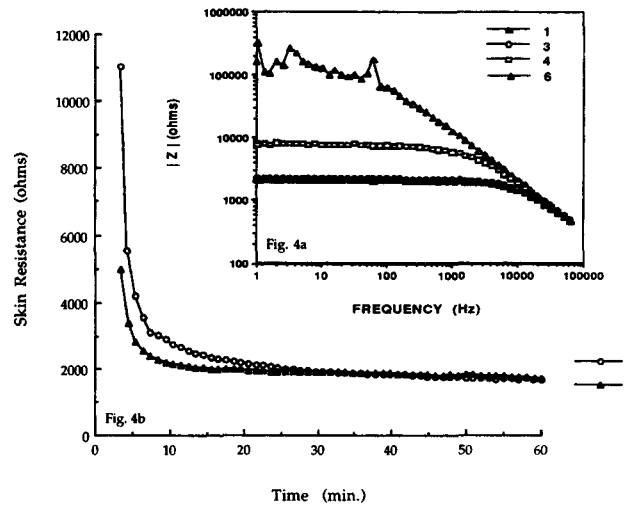

Figure 4. Impedance (a) and constant current (b) characterizations of skin resistance during on and off periods.

and rose to approximately 9,000 Ω, as shown in segment 4 of Figure 4a. When the current was reapplied, the resistance followed a different time course, but eventually reached the same steady-state value of approximately 1,800 Ω, as shown in segment 5 of Figure 4b. This steady-state resistance was also confirmed by impedance measurement, as shown in segment 6 of Figure 4a. Consequently, the steady-state resistance was reproducible for a given set of experimental conditions. Secondly, the time elapsed ($\sim 10^3$ s) to change from an equilibrium state (segment 1 of Figure 4a) to a steady state (segment 3 of Figure 4a) by the application of a constant current was much faster than the relaxation from steady state. Clearly, a rest period of 1 h only allowed a partial recovery to an intermediate resistance (segment 4 of Figure 4a) that was between the equilibrium and steady-state resistances. This result was expected since conduction and convection provided the driving forces during the application of a constant current, whereas diffusion was the primary driving force for relaxation in the absence of an applied current. Analyses of the electrical response to different external conditions will be presented in subsequent articles. The next section summarizes the effects of salt concentration (or ionic strength) and current density on the steady-state resistance of skin.

Steady-state resistance

Figures 5a and 5b show typical behavior of the steady-state resistance of skin. The current of current density on the steady-state resistances of skin in 0.012-M, 0.154-M and 1.54-M NaCl solutions are shown in Figure 5a. For a given salt concentration, the steady-state resistance of skin exhibited a nonohmic behavior, whereby it decreased with increasing current density. By replotting the data to examine the effect of salt concentration at a given current density, the steady-state resistance of skin at each current density was related to salt concentration by an exponent of approximately -0.27, as shown in Figure 5b and Table 1 for the least-square-fitted values. Data presented in the form of resistance vs. concentration also revealed the nonohmic behavior, since the resistance of a dilute salt solution is ohmic and is inversely proportional to salt concentration, as indicated by:

$$R_{\text{soln}} = \frac{L_{\text{soln}}}{F^2 z^2 (u_+ + u_-) C_o} \tag{1}$$

where R_{soln}, L_{soln}, F, z, u_+, u_-, and C_o are the solution resistance, the distance between the reference electrodes, Faraday's constant, the charge number, the mobilities of the cations and anions, and the salt concentration, respectively. Consequently, the exponent of the salt concentration would have been -1 for an ohmic resistance, but instead its value was -0.27.

The nonohmic resistance of skin could be described by several mechanisms. For instance, the lowering of resistance could arise from an increase in "pore" radius, where the aqueous pathway in skin (Cullander, 1992) was modeled by cylindrical charged pores. In such a case, the applied electrical energy would be converted to mechanical energy to expand the pore. Alternatively, if the surface of the pore was charged, such as the negative charge in human skin (Burnette et al., 1987), then the cation and anion concentrations would not be balanced

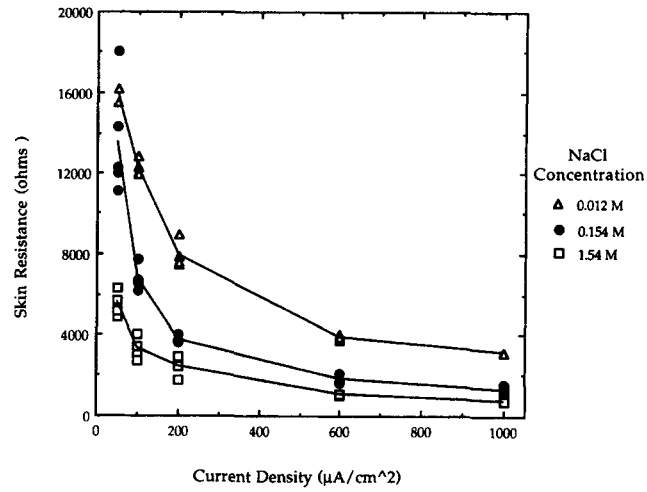

Figure 5a. Dependence of skin steady-state resistance on current density.

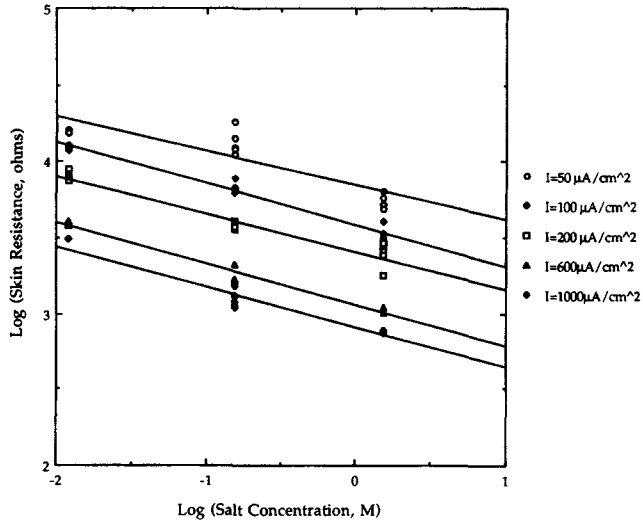

Figure 5b. Dependence on skin steady-state resistance on salt concentration.

near the surface. In this Debye layer (Probstein, 1989), an applied current would induce convective transport (Pikal, 1990, 1992) to lower the resistance. The thickness of the Debye layer (λ_D), as shown in Eq. 2, is inversely proportional to the square root of the salt concentration outside the pore, but is independent of the applied current.

$$\lambda_D = \sqrt{\frac{\epsilon RT}{2F^2 z^2 C_o}} \tag{2}$$

Table 1. Least-Squares Fitted Values: Log (Skin Resistance) = Intercept + Slope × Log (Salt Concentration)

Current Density (μA/cm^2)	Intercept	Slope
50	3.58	−0.27
100	3.84	−0.23
200	3.41	−0.25
600	3.06	−0.27
1,000	2.91	−0.27

where ϵ, R, and T are the permittivity, the gas constant, and the temperature, respectively.

The resistance data of skin, from the range of current densities examined (50-1,000 μA/cm^2), could not support a model based on a change in pore geometry. If the pore did enlarge with increasing current, then a greater fraction of the solution in the pore would be electrically neutral, since the thickness of the Debye layer would remain unchanged. Correspondingly, the dependence of the resistance of skin on salt concentration would be shifting toward an exponent of -1 as the applied current was increased. As shown in Figure 5b and Table 1, the exponent remained constant at -0.27 with increasing current density. Consequently, a change in pore geometry is an unlikely mechanism to describe the lowering in the electrical resistance of skin. Perhaps, this mechanism may exist at much higher current densities, as predicted by electroporation models (Zimmermann, 1986; Neumann and Rosenheck, 1972).

The data for the steady-state resistance of skin were analyzed by a cylindrical pore model with a constant pore radius, in which conduction and convection provided the mechanisms of transport for the ions during the application of a constant current. The analysis is outlined in the Appendix. The relationship between the steady-state resistance and the applied current density, pore geometry, salt concentration in free solution, charge density, temperature, solution dielectric constant, and solution shear viscosity is obtained from the roots of the following cubic equation:

$$\left(\frac{R}{R_{soln}}\right)^3_{steady\text{-}state}\left[\frac{\epsilon L^2_{soln}}{6\mu RTF^4z^4(u_+ + u_-)^3}\left(\frac{I}{C_o}\right)^2 f_1(\Lambda)\right] - \left(\frac{R}{R_{soln}}\right)_{steady\text{-}state}\left[1 - \frac{Fzqa}{\epsilon RT}\frac{(1-u_-/u_+)}{(1+u_-/u_+)}f_2(\Lambda) - \frac{2q^2a^2}{\epsilon RT\mu(u_+ + u_-)}f_3(\Lambda)\right] + \left(\frac{\sigma L_{sc}}{\nu L_{soln}}\right) = 0 \quad (3)$$

where R, σ, L_{sc}, ν, q, a, I, and Λ are the electrical resistance of skin, the tortuosity, the thickness of the stratum corneum, the porosity of the skin sample, the surface charge, the pore radius, the applied current density, and the ratio of the Debye thickness to the pore radius, respectively. The length of the pore is approximated by the product of the tortuosity and the thickness of the stratum corneum. The relative steady-state resistance $(R/R_{soln})_{steady\text{-}state}$ is defined by the ratio of the steady-state resistance of skin to the solution resistance. The functions $f_1(\Lambda)$, $f_2(\Lambda)$ and $f_3(\Lambda)$ are given in the Appendix. In the limiting cases of pure conduction and pure convection, the steady-state resistance can be greatly simplified and shown to be proportional to:

Conduction

$$\left(\frac{R}{R_{soln}}\right)_{steady\text{-}state} \propto \left(\frac{I}{C_o}\right)^0 \quad (4)$$

Convection

$$\left(\frac{R}{R_{soln}}\right)_{steady\text{-}state} \propto \left(\frac{I}{C_o}\right)^{-2/3} \quad (5)$$

When the applied current density is small, the dominating term is conduction. In this case, the steady-state resistance of skin is independent of current density and is directly proportional to the solution resistance which is ohmic. As the applied current density increases, convection becomes the dominant mechanism. In this case, the predicted relative resistance would be proportional to $(I/C_o)^{-2/3}$. For monovalent salts such as sodium chloride, C_o is also the concentration of the cations and the anions. The quantity I/C_o is proportional to the current carried by each ion during iontophoresis and therefore provides a measure of the process characteristic time. Accordingly, when convection dominates, the data for the steady-state resistance of skin can be consolidated into a single curve by plotting the logarithm of (skin resistance/solution resistance) vs. the logarithm of (current density/solution concentration). Consequently, the effects of current density and salt concentration on the steady-state resistance of the skin can be reduced to a master curve, as shown in Figure 6. The current density and the salt concentration ranged from 50 to 1,000 μA/cm^2 and 0.012 to 6.1 M, respectively. Each symbol denoted the resistance measured in a given salt concentration. As shown in Figure 6, a least-squares fit of the data showed that $(R/R_{soln})_{steady\text{-}state}$ is proportional to $(I/C_o)^{-0.65}$. The experimentally determined exponent of -0.65 was in excellent agreement with the theoretical value of $-2/3$, thus providing supporting evidence for the mechanism of convective transport.

Equilibrium resistance

The equilibrium electrical resistance is the electrical resistance of skin after a long period of relaxation at zero current. It is also the magnitude of the impedance which becomes independent of frequency at low frequencies. This resistance was measured by impedance spectroscopy of a skin sample that was equilibrated in a salt solution for 24 h. As shown in Figure 4a, the equilibrium resistance, which was measured for a fresh skin sample, was approximately two orders of magnitude higher than the steady-state resistance at an applied current density of 600 μA/cm^2 in 0.154-M NaCl. However, the equilibrium resistance could be very sensitive to the porosity of the skin

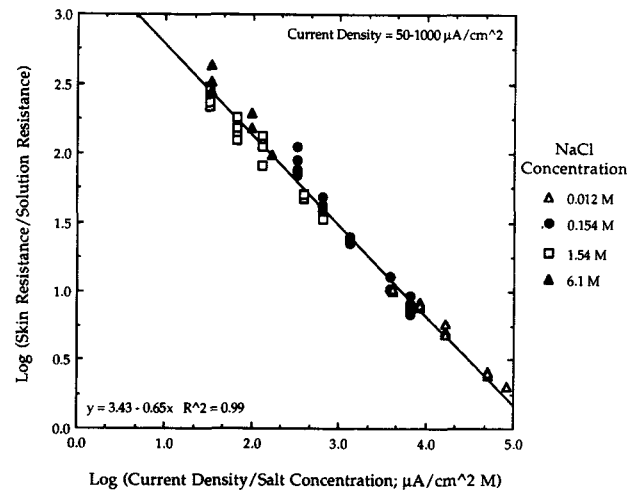

Figure 6. Effects of current density and salt concentration on skin and solution resistances.

Table 2. Equilibrium Electrical Resistance of Skin as a Function of Salt Concentration

Salt Conc. (M)	Solution Res. (Ω)	Equilib. Skin Res. (Ω)	Equilib. Rel. Resist.
0.012	1,539	583,179	379
0.154	161	330,434	2,052
1.54	22	60,114	2,732

sample and the geometry of the pores and therefore could be subjected to variabilities within and between skin donors. For skin samples with wide pores, the equilibrium resistance of skin would be proportional to the solution resistance. The proportionality constant would then be a function of the porosity and geometrical factors. As an example, one set of data reported by DeNuzzio and Berner (1990) showed that the resistance of skin was approximately ten times greater than the solution resistance. More generally, the equilibrium resistance is a nonlinear function of salt concentration, as illustrated by a typical set of equilibrium resistance data measured in various salt concentrations using a single skin donor. Table 2 and Figure 7 show that the relative equilibrium resistance, which is the ratio of the equilibrium resistance of skin to the solution resistance, increased with increasing salt concentration. This result is due to a thinning of the Debye layer with increasing salt concentration in free solution, outside of the pores of the skin. The equilibrium resistance is made up of contributions from the Debye layer and from the core. The resistance in the Debye layer is lower, due to higher ion concentrations than the resistance in the core, which is the same as the resistance of a salt in free solution. Consequently, the equilibrium relative resistance increases with increasing salt concentration, because the contribution from a thinner Debye layer decreases.

A model was developed relating the equilibrium relative resistance to the structural properties of skin and is given by:

$$\left(\frac{R}{R_{\text{soln}}}\right)_{\text{equilibrium}} = \left(\frac{\sigma L_{sc}}{\nu L_{\text{soln}}}\right)\left[1 - \frac{Fzqa}{\epsilon RT}\frac{(1-u_-/u_+)}{(1+u_-/u_+)} f_2(\Lambda) - \frac{2q^2a^2}{\epsilon RT\mu(u_+ + u_-)} f_3(\Lambda)\right]^{-1} \quad (6)$$

For the data shown in Figure 7, the estimated pore radius, the surface charge, $(\sigma L_{sc}/\nu L_{\text{soln}})$, and the ratio of porosity to tortuosity of a pore were 25×10^{-10} m, $q = -0.05$ C/m^2, 2,800, and 10^{-7} for the skin sample used in the experiment, respectively. Although a model consisting of cylindrical pores is a highly simplified representation of the aqueous pathway in skin, it is interesting to note that the estimated pore radius of 25×10^{-10} m is within the same order of magnitude as the average radius of 18×10^{-10} m reported by Inamori et al. (1992) for human skin and Ruddy et al. (1992) for hairless mouse skin. Yoshida and Roberts (1992) also estimated a pore radius of 30×10^{-10} m for human skin. The magnitude of the ratio of porosity to tortuosity suggests that the void fraction of the pathways for ion transport across skin is much smaller than the area fraction of the appendages. Additional independent measurements would be required to determine the tortuosity and the porosity separately.

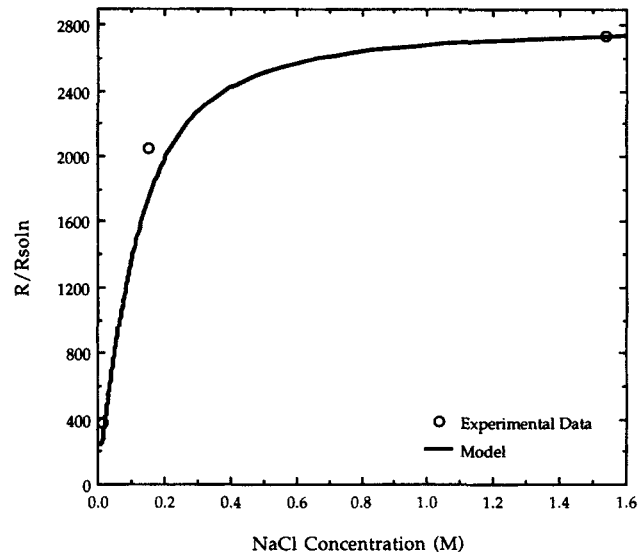

Figure 7. Effect of salt concentration on skin equilibrium and solution resistances.

Conclusions

This work focused on characterizing the electrical properties of skin. The electrical resistance of skin was shown to be bound by an upper limit at equilibrium and a lower limit at steady state. During the application of a constant current, the time to reach steady state was approximately 10^3 s. In contrast, the recovery to equilibrium by diffusion requires a much longer time.

The equilibrium resistance was measured by impedance spectroscopy of a fresh skin sample that was equilibrated in a salt solution. The equilibrium resistance was sensitive to the variability in skin samples, due to its dependence on the porosity of the sample and the geometry of the pores. For skin samples with wide pores, the equilibrium resistance approached a value that was proportional to the resistance of the free salt solution. In general, the equilibrium relative resistance, which is the ratio of the resistances of skin to solution, increased with increasing salt concentration. A model was developed relating the equilibrium relative resistance to the structural properties of skin. The estimated pore radius of 25×10^{-10} m from the equilibrium resistance data is consistent with the average pore radius of human skin reported in the literature.

In the presence of a constant current, the resistance of skin decreased precipitously from its equilibrium value to a steady-state value. This difference can greatly reduce the power requirement for iontophoresis and can make this novel technology more practical. The steady-state resistance, which depended on both current density and salt concentration, had a specific value that was independent of a skin sample prior exposures to a current. For the range of experimental conditions examined (0.012–6.1-M NaCl solution, and 50–1,000 μA/cm^2), a linear relationship was found between the logarithm of the steady-state relative resistance and the logarithm of the current density divided by the salt concentration. The slope of -0.65 was in excellent agreement to a theoretical value of $-2/3$, which was derived for the convective transport of ions in a charged pore under a constant current.

Iontophoresis and controlled-release technology are aimed

at providing solutions to unmet medical needs. Beyond the problem of drug input are the issues of drug distribution, metabolism and excretion. These are intriguing and challenging topics for fundamental research in chemical engineering.

Acknowledgment

We would like to acknowledge Mr. Avinash Agarwal and Ms. Deborah Kachmar for their assistance.

Notation

a = pore radius, m
c_k = concentration of species k, M
C_o = salt concentration, M
C_+ = cation concentration, M
C_- = anion concentration, M
F = Faraday's constant, 9.648×10^4 C/mol
$f_1(\Lambda)$ = function defined by Eq. 4
$f_2(\Lambda)$ = function defined by Eq. 5
$f_3(\Lambda)$ = function defined by Eq. 6
I = applied current density, A/m^2
I_0 = modified Bessel function of order 0
I_1 = modified Bessel function of order 1
L_{sc} = thickness of stratum corneum, m
L_{soln} = distance between reference electrode, m
q = surface charge, C/m^2
r = radial position
R = gas constant, 8.314 J/(K mol)
R = electrical resistance of skin
R_{soln} = electrical resistance of salt solution
T = temperature, K
u_+ = mobility of cation, mol·m^2/(J·s)
u_- = mobility of anion, mol·m^2/(J·s)
v_x = axial velocity, m/s
x = axial position
z = charge number

Greek letters

ϵ = permittivity, C/(V m)
λ_D = Debye thickness, m
Λ = ratio of Debye thickness to pore radius
μ = shear viscosity, Pa·s
ν = porosity
ρ_E = charge density, C/m^3
σ = tortuosity
ϕ = potential, V
ϕ_o = potential at the centerline of a pore, V
Φ_{in}-Φ_{out} = radially-averaged potential difference across the length of a pore, V

Literature Cited

Berner, B., and S. M. Dinh, "Fundamental Concepts in Controlled Release," *Treatise on Controlled Drug Delivery*, A. Kydonieus, ed., Marcel Dekker, New York, p. 1 (1992).
Burnette, R. R., and B. Ongpipattanakul, "Characterization of the Permselective Properties of Excised Human Skin During Iontophoresis," *J. Pharm. Sci.*, **76**, 765 (1987).
Coster, H. G. L., K. J. Kim, K. Dahlan, J. R. Smith, and C. J. D. Fell, "Characterization of Ultrafiltration Membranes by Impedance Spectroscopy: I. Determination of the Separate Electrical Parameters and Porosity of the Skin and Sublayers," *J. Memb. Sci.*, **66**, 19 (1992).
Cullander, C., "What are the Pathways of Iontophoretic Current Flow Through Mammalian Skin?," *Adv. Drug. Del. Rev.*, **9**, 119 (1992).
DeNuzzio, J. D., and B. Berner, "Electrochemical and Iontophoretic Studies of Human Skin," *J. Controlled Release*, **11**, 105 (1990).
Foley, D., J. Corish, and O. I. Corrigan, "The Effect of Iontophoresis on the Electrical and Transport Properties of Human Epidermal Tissue," *Prediction of Percutaneous Penetration*, Vol. 2, p. 420, IBC Technical Services, Oxford, UK (1991).
Inamori, T., A. H. Ghanem, and W. I. Higuchi, "Estimation of Pore Size of Ethanol Pretreated Human Epidermal Membrane Using Polystyrene Sulfonate," *Proc. Int. Symp. Control. Rel. Bioact. Mater.*, **19**, 474 (1992).
Kasting, G. B, and L. A. Bowman, "DC Electrical Properties of Frozen, Excised Human Skin," *Pharm. Res.*, **7**, 134 (1990).
MacDonald, D. D., *Transient Techniques in Electrochemistry*, Plenum Press, New York, p. 229 (1981).
Michaels, A. S., S. K. Chandrasekaran, and J. E. Shaw, "Drug Permeation Through Human Skin: Theory and *In Vitro* Experimental Measurement," *AIChE J.*, **21**, 985 (1975).
Mostowski, A., and M. Stark, *Introduction to Higher Algebra*, Pergamon Press, Oxford, p. 291 (1964).
Neumann, E., and K. Rosenheck, "Permeability Changes Induced by Electric Impulses in Vesicular Membranes," *J. Memb. Biol.*, **10**, 279 (1972).
Pikal, M. J., "Transport Mechanism in Iontophoresis: I. A Theoretical Model for the Effect of Electroosmotic Flow on Flux Enhancement in Transdermal Iontophoresis," *Pharm. Res.*, **7**, 118 (1990).
Pikal, M. J., "The Role of Electroosmotic Flow in Transdermal Iontophoresis," *Adv. Drug. Del. Rev.*, **9**, 201 (1992).
Probstein, R. F., *Physiochemical Hydrodynamics*, Butterworths, Boston, p. 187 (1989).
Ruddy, S. B., and B. A. Hadzija, "Iontophoretic Permeability of Polyethylene Glycols Through Hairless Rat Skin: Application of Hydrodynamic Theory for Hindered Transport Through Liquid-Filled Pores," *Drug Des. Discovery*, **8**(3), 207 (1992).
Scheuplein, R. J., and I. H. Blank, "Permeability of the Skin," *Physiological Rev.*, **51**(4), 702 (1971).
Tregear, R. T., *Physical Functions of Skin*, Academic Press, London, p. 66 (1966).
Yoshida, N. H., and M. S. Roberts, "Structure-Transport Relationships in Transdermal Iontophoresis," *Adv. Drug Del. Rev.*, **9**, 239 (1992).
Zimmermann, U., "Electrical Breakdown, Electropermeabilization and Electrofusion," *Rev. Physiol. Biochem. Pharmacol.*, **105**, 175 (1986).

Appendix: Ion Transport Analysis in a Charged Pore under a Constant Current

The derivation of Eq. 3 for the relative resistance, R/R_{soln}, is outlined below. A charged pore for the transport of ions is shown in Figure A1. The applied current density, I, is determined from the radially-averaged axial current density and at steady-state it is given by:

$$\frac{I}{\nu} = \frac{2F^2}{a^2}\sum_k \left[z_k^2 u_k \int_0^a c_k \left(-\frac{\partial \phi}{\partial x} \right) r dr \right] + \frac{2}{a^2}\int_0^a r v_x \rho_E dr \qquad \text{(A1)}$$

where c_k, ϕ, x, r, v_x, $\rho_E (\equiv F\Sigma_k z_k c_k)$ are the concentration of species k, the potential, the axial direction, the radial direction, the axial velocity, and the charge density, respectively. Note

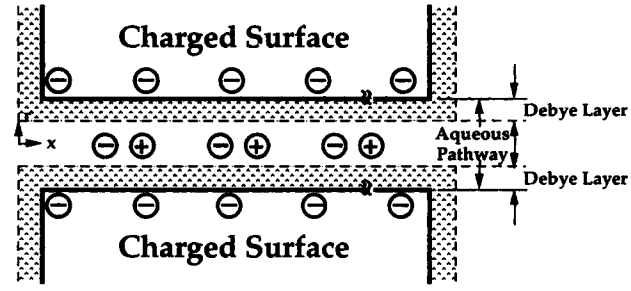

Figure A1. Pore model of ion transport across a charged pore under a constant current.

that the diffusive term in the axial direction has been omitted. Clearly, the concentration of each species, the potential and the axial velocity need to be related to the radial position. For a binary salt, the Boltzman relationship between concentration and potential is obtained by assuming equilibrium for the radial component of flux and electrical neutrality in the centerline of the pore. The Debye-Hückel approximation is simply the linearized result, which is given by:

$$c_{\pm} = C_o\left[1 \mp \frac{zF}{RT}(\phi - \phi_o)\right] \tag{A2}$$

where c_+, c_-, and ϕ_o are the concentrations of cations and anions, and the potential at the centerline of a pore, respectively. The potential is then related to the radial position by Poisson's equation:

$$\frac{1}{r}\frac{\partial}{\partial r}\left(r\frac{\partial \phi}{\partial r}\right) = -\frac{\rho_E}{\epsilon} \tag{A3a}$$

with the boundary conditions of symmetry at the center-line, and of overall charge neutrality between the electrolyte and the pore surface charge:

$$r = 0, \quad \frac{\partial \phi}{\partial r} = 0 \tag{A3b}$$

and

$$r = a, \quad 2\pi\int_0^L\int_0^a \rho_E r dr dx = -2\pi aqL \tag{A3c}$$

The axial velocity is obtained from the axial component of the momentum equation, which is given by:

$$0 = \frac{\mu}{r}\frac{\partial}{\partial r}\left(r\frac{\partial v_x}{\partial r}\right) + \rho_E\left(-\frac{\partial \phi}{\partial x}\right) \tag{A4a}$$

with the boundary conditions of symmetry at the centerline, and of no-slip at the pore surface:

$$r = 0, \quad \frac{\partial v_x}{\partial r} = 0 \tag{A4b}$$

and

$$r = a, \quad v_x = 0 \tag{A4c}$$

where μ is the shear viscosity of the electrolyte. The boundary conditions for the potentials at the inlet and outlet of the pore are determined by their radially-averaged values. The radially-averaged potential difference across the length of the pore, $(\Phi_{in} - \Phi_{out})$, is measurable and is defined by:

$$\Phi_{in} - \Phi_{out} = \frac{2}{a^2}\int_0^a [\phi(r, x=0) - \phi(r, x=L)] r dr \tag{A5}$$

The expression for the relative steady-state resistance (Eq. 3) is derived by combining Eqs. A1 to A4, where the resistance is defined by the ratio of the radially-averaged potential difference across the length of the pore to the applied current, and the functions $f_1(\Lambda)$, $f_2(\Lambda)$ and $f_3(\Lambda)$ in Eq. 3 are given by:

$$f_1(\Lambda) = \frac{2\Lambda^2}{\left[1 - 2\Lambda\dfrac{I_1(1/\Lambda)}{I_0(1/\Lambda)}\right]^3}\left\{\int_0^{1/\Lambda} y\frac{I_0(y)}{I_0(1/\Lambda)} \times \int_{1/\Lambda}^{y}\frac{1}{y'}\int_0^{y'} y''\frac{I_0(y'')}{I_0(1/\Lambda)}\left[1 - \frac{I_0(y'')}{I_0(1/\Lambda)}\right] dy'' dy' dy\right\} \tag{A6}$$

and

$$f_2(\Lambda) = \frac{2\Lambda^3\dfrac{I_0(1/\Lambda)}{I_1(1/\Lambda)}}{\left[1 - 2\Lambda\dfrac{I_1(1/\Lambda)}{I_0(1/\Lambda)}\right]} \times \left\{\int_0^{1/\Lambda} y\frac{I_0(y)}{I_0(1/\Lambda)}\left[1 - \frac{I_0(y)}{I_0(1/\Lambda)}\right] dy\right\} \tag{A7}$$

and

$$f_3(\Lambda) = \frac{2\Lambda^4\left(\dfrac{I_0(1/\Lambda)}{I_1(1/\Lambda)}\right)^2}{1 - 2\Lambda\dfrac{I_1(1/\Lambda)}{I_0(1/\Lambda)}}\left\{\int_0^{1/\Lambda} y\frac{I_0(y)}{I_0(1/\Lambda)}\int_{1/\Lambda}^{y}\frac{1}{y'} \times \int_0^{y'} y''\frac{I_0(y'')}{I_0(1/\Lambda)}\left[1 - \frac{I_0(y'')}{I_0(1/\Lambda)}\right] dy'' dy' dy\right\} \tag{A8}$$

where I_0 and I_1 are the modified Bessel functions of order 0 and 1, respectively. The steady-state resistance can then be explicitly determined by applying Cardan's formula (Mostowski and Stark, 1964) for the roots of a cubic equation (Eq. 3).

Manuscript received Feb. 19, 1993, and revision received Apr. 26, 1993.